Methane oxidation minimizes emissions and offsets to carbon burial in mangroves

Luiz Cotovicz, Gwenaël Abril, Christian Sanders, Douglas Tait, Damien Maher, James Sippo, Ceylena Holloway, Yvonne Yau, Isaac Santos

Title

Methane oxidation minimizes emissions and offsets to carbon burial in mangroves

Author list

Luiz C. Cotovicz Jr.[1,2,*]; Gwenaël Abril[3,4]; Christian J. Sanders[5]; Douglas R. Tait[5,6]; Damien T. Maher[6]; James Z. Sippo[6]; Ceylena Holloway[5]; Yvonne Y. Y. Yau[7]; Isaac R. Santos[5,7]

Affiliations

1 Department of Marine Chemistry, Leibniz Institute for Baltic Sea Research, Warnemünde, Germany

2 Instituto de Ciências do Mar (LABOMAR), Universidade Federal do Ceará, Fortaleza, Brazil

3 Laboratoire de Biologie des Organismes et Ecosystèmes Aquatiques (BOREA), UMR 8067, Muséum National d'Histoire Naturelle, CNRS, IRD, SU, UCN, UA, Paris, France

4 Programa de Pós-Graduação em Geociências, Universidade Federal Fluminense, Brazil

5 National Marine Science Centre, Southern Cross University, Coffs Harbour, Australia

6 Faculty of Science and Engineering, Southern Cross University, Lismore, Australia

7 Department of Marine Sciences, University of Gothenburg, Gothenburg, Sweden

*corresponding author: luiz.cotovicz@io-warnemuende.de

Abstract

Maximizing carbon sequestration in mangroves is part of the global effort to combat the climate crisis. However, methane (CH_4) emissions can partially offset carbon sequestration in mangroves. Previous estimates suggested that CH_4 emissions offset organic carbon burial by 20% in mangroves with significant freshwater inputs and/or highly impacted. Here, we resolve the magnitude and drivers of the mangrove CH_4 offset using multiple isotopic tracers across a latitudinal gradient. CH_4 emission offsets were smaller in high salinity (~7%) than freshwater-influenced (~27%) mangroves. Carbon sequestration was disproportionally high compared to CH_4 emissions in understudied tropical areas. Low CH_4 emissions were explained by minor freshwater inputs minimizing CH_4 production in saline, high sulphate conditions and intense CH_4 oxidation in porewaters and surface waters. CH_4 oxidation in mangrove surface waters reduced potential aquatic CH_4 emissions by 10-33%. Overall, carbon sequestration through mangrove preservation and restoration is less affected by CH_4 emissions than previously thought.

Main text

Mangroves are a blue carbon ecosystem with high productivity and carbon sequestration efficiency[1,2]. Enhancing mangrove carbon sequestration has been suggested as a nature-based solution to climate change[3]. The major pathways of mangrove carbon fluxes have been quantified during the past decade. Primary production in global mangroves is 218 ± 72 Tg C yr^{-1} [4,5]. Much of this carbon is exported to the ocean as dissolved carbon following tidal flushing of intertidal soils [4,6,7]. A further large partion is recycled and emitted as carbon dioxide (CO_2) to the atmosphere (34.1 ± 5.4 Tg C yr^{-1}) [8]. A similar quantity of organic carbon (41 Tg C yr^{-1}) is buried in sediments[9]. The buried organic carbon in mangroves consists predominantly of autochthonous sources mixed with minor allochthonous sources[10] that are preserved due to the anoxic sediment conditions[11]. However, major components of mangrove carbon cycling such as CH_4 emissions remain poorly resolved.

Mangroves release methane (CH_4) to the atmosphere following organic matter degradation in sediments[12–14]. Accounting for CH_4 emissions is important to resolve net carbon sequestration because CH_4 is a 45-96 times more powerful greenhouse gas than CO_2 on a mass basis, considering the sustained-flux global warming potential (SGWP) for 100-year and 20-year time horizons, respectively[15]. Recent investigations questioned the blue carbon benefits of mangroves due to the high global warming potential of methane emissions[14,16–18]. Some studies suggested that the methane emissions can partially[14,19] or fully counteract[16] the climatic benefits of mangrove carbon burial. Estimated methane emission offsets of 17-23%[14] have large, unknown uncertainties because they are based on limited data in deltaic and estuarine mangroves that receive methane-enriched freshwater inputs. This freshwater can lead to a misassignment of CH_4 emissions to mangroves when in reality methane may come from upstream sources[20]. Furthermore, the in situ production of CH_4 is significant in freshwater-dominated mangroves[20]. The lack of data in seawater-dominated mangrove ecosystems prevents reasonable global estimates of CH_4 emissions.

The rate of CH_4 oxidation is another key process regulating CH_4 emissions. Tidal flushing supplies oxygen to organic-rich sediments, oxidizing organic matter and releasing nutrients and CO_2[5,21,22]. Large amounts of CH_4 can be oxidized to CO_2 in lakes and the ocean before it reaches the atmosphere[23,24]. However, CH_4 oxidation has rarely been quantified in mangrove ecosystems[25]. If oxidation is significant, CH_4 emissions could be significantly reduced with climate consequences at geological and contemporary time-scales[26]. The fractionation of ^{13}C during methanogenesis leads to depleted $\delta^{13}C$ signatures of CH_4, whereas ^{13}C fractionation during oxidation gradually increases residual $\delta^{13}C$[27,28]. It is essential to document CH_4 oxidation rates in mangroves to resolve whether it minimizes CH_4 emissions.

Here, we resolve mangrove CH_4 emissions, oxidation and offsets to the net radiative forcing associated with organic carbon burial in sediments across a latitudinal gradient including understudied tropical mangroves (Extended Data Fig. 1, Supplementary Information Table S1-S7). We then combine our new observations with earlier datasets to reevaluate global estimates of mangrove methane emissions. We hypothesize that previous estimates of aquatic CH_4 emissions from mangroves are overestimated due to an observation bias towards freshwater-influenced mangroves. Our observations reveal that oxidation minimizes CH_4 emissions as an offset to carbon burial in mangroves. Global upscaling with our new observations showed that methane emissions in seawater-dominated mangroves are ~14 times lower than in freshwater-influenced mangroves, requiring a reevaluation of mangrove carbon budgets.

Salinity controls mangrove CH_4 emissions

High resolution observations of dissolved CO_2 and CH_4 concentrations and $\delta^{13}C$ signatures in six seawater-dominated mangrove creeks across a latitudinal gradient revealed clear tidal cycles

(Extended Data Figs. 2-5). Tidal flushing of porewater enriched with products of organic matter degradation explains higher CH_4 concentrations and lighter $\delta^{13}C$ signatures during low tide than high tide [22,29,30]. Indeed, CH_4 concentrations exhibited positive correlations with radon (^{222}Rn, a natural porewater tracer) in all mangrove creeks (Extended Data Fig. 6), providing further evidence that porewater is the dominant CH_4 source.

Previous estimates of CH_4 emissions from mangrove waters focused on ecosystems receiving large amounts of freshwater (Fig. 1A) [5,14,31]. Maximum CH_4 is generally observed in periods of high freshwater discharge[14,32]. However, freshwater-influenced mangroves can shift to seawater-dominated conditions during dry conditions[32]. Here, we quantify emissions from mangroves with salinity >30. Hence, our observations mostly represent mangrove ecosystems rather than upstream freshwater sources (Fig. 1A). Dissolved CH_4 concentrations in seawater-dominated mangroves (42 ± 34 nmol L^{-1}) were much lower than previous observations in freshwater-influenced mangroves. Our new observations lower the global average of 245 ± 49 nmol L^{-1}, as reported across nine systems[33], to 143 ± 59 nmol L^{-1} based now on fifteen mangrove sites. The ranges of aquatic CH_4 emissions in our latitudinal transect (40.3 ± 2.7 to 137.2 ± 3.2 μmol m^{-2} d^{-1}) are 15-47% of earlier observations in freshwater-influenced mangrove ecosystems (288.0 ± 73.2 μmol m^{-2} d^{-1}, [14]). While CH_4 concentrations and emissions in freshwater-influenced mangroves have pronounced seasonal variability[14,32], seawater-dominated mangroves have minor seasonality due to the major influence of oceanic water and minor freshwater inputs[34,35].

Overall, the relationship between CH_4 and salinity in all local-scale studies (Fig. 1) further supports our suggestion that earlier global estimates of methane emissions from mangroves were overestimated due to freshwater inputs. Higher CH_4 emissions in mangroves receiving freshwater can be explained by (1) substantial external CH_4 inputs from rivers or upstream freshwater wetlands[36]; and (2) enhanced *in situ* methanogenesis in systems with low sulphate concentrations and high organic matter[37–39]. The positive relationship between CH_4 emissions and carbon dioxide (CO_2) (Fig. 1B) and the natural tracer radon (^{222}Rn) (Extended Data Fig. 6) indicates an analogous porewater source. However, the steeper slope of CO_2 to CH_4 for brackish mangroves (Fig. 1B) implies reduced CH_4 production when seawater sulphate is available[37]. Indeed, the lowest emissions of CH_4 and CO_2 were reported in arid, carbonate mangroves exhibiting the highest salinities[40] and in our seawater-dominated mangroves.

In addition to the water-atmosphere diffusive fluxes quantified here, there are other potential CH_4 emission pathways in mangroves, including soil-atmosphere[20], plant-mediated transport[41,42], and water-atmosphere ebullitive fluxes[12]. The few investigations of CH_4 emissions by emerged mangrove soils revealed values similar or lower than aquatic emissions (59.3 ± 93.0 μmol m^{-2} d^{-1})[13,34]. The strong negative relationship between soil-atmosphere emissions of CH_4 and salinity suggests similar controlling factors and low emissions in high salinity mangroves[20]. Plant-mediated CH_4 emissions remain understudied[41–43]. Living mangrove tree-stems[41] can release 37.5 ± 5.8 μmol m^{-2} d^{-1} of CH_4 but plants can also act as CH_4 sinks depending on salinity and microbial activity[42]. Ebullitive fluxes of CH_4 may be significant in freshwater-dominated, polluted mangroves[12,44,45,46]. In some degraded freshwater-influenced Indian mangroves, CH_4 emissions via ebullition (30 to 190 μmol m^{-2} d^{-1}) negatively correlated to salinity[45]. Bubble formation in marine sediments may occurs below the sulfate depletion depth[26], however, in seawater-dominated mangroves, this zone is likely constrained to deeper sediment layers[47]. In coastal sediments, CH_4 ebullition is tightly coupled to the variation of the tidal height and occurs almost exclusively around low tide when freshwater reaches mangroves[48] and due to a reduction in hydrostatic pressure[49]. However, no studies have demonstrated bubble ebullition as a significant CH_4 release pathway in high salinity, pristine mangrove systems.

Increasing sulfate concentration with salinity offers an ample source of electron acceptors for sulfate-reducing bacteria that outcompete methanogens for substrate[50]. Therefore, methanogenesis occurs in deep, anoxic layers of the sediment[51]. Anaerobic oxidation of methane coupled to sulfate reduction can also occur in anoxic marine sediments, representing an important CH_4 sink[51,52]. The amount of CH_4 escaping anaerobic oxidation in deep layers diffuses to the upper sediment layers,

where it can be partially oxidized by methanotrophs[53]. In freshwater sediments, organic matter mineralization can be dominated by methanogenesis[54]. However, in coastal marine systems, tidal pumping supplies sulphate and oxygen that inhibit methanogenesis[55]. Indeed, CH_4 fluxes are significantly reduced at salinities >15[39,54,56,57], and CH_4 production can be reduced by ~94% in marine sediments compared to freshwater sediments[57]. The relationship between salinity and dissolved CH_4 established in local studies[39,58,59] clearly holds on a global scale (Fig. 1) with major implications to how we interpret the role of mangroves as carbon sinks. Including upstream freshwater sources clearly overestimates the role of methane as an offset to mangrove carbon sequestration.

Small CH_4 offset to mangrove carbon sequestration

Earlier observations in mangroves influenced by freshwater suggested that aquatic emissions of CH_4 offset ~20% of the net radiative forcing benefit of organic carbon sequestration in mangrove sediments[14]. However, this potential offset was based on 24-h time series observations in three freshwater-influenced mangroves combined with earlier data from six other freshwater-influenced and often anthropogenically-impacted mangroves. These previous studies also used global averages of carbon burial rates rather than local estimates to define the CH_4 offset. Our longer observations focusing on six seawater-dominated mangroves across a broad latitudinal gradient with locally estimated burial rates (Supplementary Information Table S4, S5, Fig. S7) revelead an average CH_4 offset of only 9% (Fig. 2A). This offset decreases further to 8% if we consider nitrous oxide (N_2O) uptake in nitrogen-limited mangrove creeks[60] (Supplementary Information Table S7). The N_2O sink and smaller CH_4 source in seawater-dominated mangroves are a clear contrast to mangroves influenced by freshwater inputs and pollution.

Carbon burial and biomass increase towards the tropics where most mangroves occur[9,61,62]. The lowest CH_4 offset (2.2%) and highest rate of organic carbon burial (216 ± 17 g C m^{-2} yr^{-1} or 791 g CO_2 m^{-2} yr^{-1}) occurred in the tropics (Fig. 2A,B). This sequestration rate compares well with the global average of 194 ± 15 g C m^{-2} yr^{-1} (or 711 g CO_2 m^{-2} yr^{-1})[9]. Our most tropical mangrove system had large tidal variability and deeper waters (4.3 m, Supplementary Information Table S1) that favor CH_4 oxidation and minimize CH_4 emissions[63]. Freshwater-influenced mangroves also have the lowest offset (1.4%) in the tropics[14]. Therefore, the ratio of organic carbon burial to CH_4 emissions are much higher in understudied tropical mangroves. Interestingly, our average rate of organic carbon burial (102 ± 66 g C m^{-2} yr^{-1} or 374 g CO_2 m^{-2} yr^{-1}) in the six mangroves nearly matches a recent mean global estimation of carbon burial for open coast and lagoon mangrove biophysical types (103 g C m^{-2} yr^{-1} or 377 g CO_2 m^{-2} yr^{-1}, [64]). The highest offset (latitude 32° S) coincided with the lowest average organic carbon burial (50 ± 6 g C m^{-2} yr^{-1} or 293 g CO_2 m^{-2} yr^{-1}). Even our maximal aquatic CH_4 offset (~17%) is lower than earlier global averages biased by freshwater methane.

Previous estimates of high CH_4 offsets[14] relied on several major assumptions. First, all emissions were assumed to be due to mangroves rather than upstream freshwater inputs. Mangroves with low freshwater influence emits less CH_4 (Fig. 1A,B) but represent >32% of the global mangrove area[65]. A new global mangrove typology shows that 40.5% of mangrove systems are deltaic, 27.5% are estuarine, 21.0% are open coast, and 11.0% are lagoonal[65]. We consider that seawater-dominated mangroves include lagoonal and open coast types. However, even deltaic and estuarine mangroves include regions with salinity >30, and freshwater-influenced mangroves can be dominated by seawater during low flow conditions[32]. For instance, mangroves on the Amazon delta are all classified as deltaic, but several areas have tidal creeks with salinity >30 [29]. Second, local CH_4 emissions were compared to global rates of organic carbon burial[14]. We did not find a significant link between CH_4 emissions and organic carbon burial (Fig. 2B). This implies that CH_4 offsets to organic carbon burial is site-specific. The rates of mangrove organic carbon burial and aquatic CH_4 emissions can span over three orders of magnitude[31,64]. Therefore, comparing local estimates of CH_4 emissions with the global

196 average of organic carbon burial introduces biases due to different spatial representations of each
197 carbon pathway. Hence, considering pristine seawater-dominated systems increases mangrove's net
198 global radiative forcing benefit.

199

200 ***CH_4 oxidation minimizes CH_4 emissions***

201 We also reveal how CH_4 oxidation in mangrove porewater and surface water reduces potential
202 CH_4 emissions (Extended Data Fig. 3). Fractionation during oxidation enriches the heavier isotope in
203 the residual CH_4[26,27]. Our measured CH_4 isotope values in porewaters were less negative than the
204 theoretical source calculated from surface creek water data using keeling plots and a conservative
205 mass balance (referred to here as the conservative $\delta^{13}C$-CH_4 in porewater, Fig. 3A). This implies CH_4
206 oxidation in porewater. $\delta^{13}C$-CH_4 in porewaters reached a maximal enrichment of 27‰ in subtropical
207 mangroves compared to a porewater end-member theoretical signature of –80‰ to –65‰. The low
208 CH_4 concentrations in ^{13}C-enriched shallow porewaters further implies oxidation is taking place
209 (Supplementary Information Fig. S5). Porewater $\delta^{13}C$-CH_4 was occasionally heavier than creek water
210 at low tide, implying the mobilization of deeper porewater with tidal pumping.

211 High organic carbon deposition rapidly consumes O_2, minimizing aerobic methane
212 oxidation[66]. The mean $\delta^{13}C$-CH_4 value in porewater was negatively correlated to the mean organic
213 carbon burial (Fig. 3B). However, data clustered in two groups. Despite a significant correlation, these
214 results should be interpreted with caution. The mean $\delta^{13}C$-CH_4 value in porewater was also negatively
215 correlated to porewater exchange rates (Fig. 3C). Surface water penetrates sediments on tidal time
216 scales[67]. Hence, rapid porewater exchange likely prevents some CH_4 oxidation due to the short
217 residence time. Rapid porewater flushing would transfer methane to surface waters prior to oxidation.
218 The geomorphic and sedimentary settings[65] and the physiognomy[68] of mangroves drive water
219 residence time[53], which influences CH_4 production, oxidation and dispersion (outwelling).

220 The fraction of CH_4 oxidation in surface waters could be calculated only for the two tropical
221 mangroves where the observed and the calculated conservative $\delta^{13}C$-CH_4 signatures matched the
222 signature observed in porewater (Fig. 3A, 3D). The fraction of CH_4 oxidation in tidal creek water was
223 highest in the most tropical mangrove Darwin at 12°S (34 ± 11%) where low CH_4 concentrations in
224 surface waters were linked to high oxidation (Fig. 3D). CH_4 oxidation within the water column was
225 likely a result of oxygen-rich seawater inputs[69]. Maximal rates of CH_4 oxidation in Darwin are related
226 to a large tidal range and deep waters (~8 m). Deeper water increases the residence time of CH_4 and
227 therefore favors oxidation versus emission[63]. CH_4 oxidation in Darwin averaged 20.9 ± 8.9 μmol m^{-2}
228 d^{-1}, about half of the CH_4 outgassing (40.5 ± 2.0 μmol m^{-2} d^{-1}). Methane oxidation at Hinchinbrook
229 Island (18°S) (15.3 ± 2.7 μmol m^{-2} d^{-1}) was equivalent to about 10% of CH_4 outgassing (137.9 ± 3.2
230 μmol m^{-2} d^{-1}). This large natural variability highlights the importance of site-specific measurements of
231 CH_4 oxidation.

232 Overall, we reveal that CH_4 oxidation in high salinity mangroves minimizes the potential for
233 aquatic CH_4 emissions. In saline, arid Mexican mangroves, low concentrations of CH_4 in porewaters
234 (<30 nmol L^{-1}) were due to anaerobic oxidation rather than the inhibition of methane production by
235 sulfate reducers[25]. Very few studies have quantified CH_4 oxidation in freshwater-influenced
236 mangroves[70–72]. In freshwater-influenced mangroves of the Sundarbans, average CH_4 oxidation in
237 surface water was 20.6 nmol L^{-1} d^{-1} (or 72.1 μmol m^{-2} d^{-1} for a water column depth of 3.5 m) [70]. This
238 rate is 3-4 times higher than observed in our seawater-dominated mangroves. Sundarbans sediments
239 have strong oxidation in the aerobic zone with steep vertical gradients from 20 μmol m^{-2} d^{-1} at 60 cm
240 to 3380 μmol m^{-2} d^{-1} at the surface oxic soil [72]. CH_4 oxidation in Sundarbans removed ~40% of the
241 total CH_4 produced in sediments[71]. In high salinity, pristine Mexican mangroves, oxidation removed
242 about 80% of the total CH_4 produced[25]. Our data revealed average oxidation rates in surface water of

tidal creeks ranging between 10% and 35%. Further research research is needed to resolve the scale of CH_4 production and oxidation in mangroves influenced by freshwater and those dominated by seawater, both in sediments/porewaters and in surface waters.

Implications

Methane emissions and the carbon budget of saline, pristine mangroves are significantly different from those in the previously studied freshwater-influenced and sometimes anthropogenically impacted mangrove ecosystems[5,14]. High upstream CH_4 inputs and low sulfate explain higher CH_4 emissions in freshwater-influenced mangroves. CH_4 oxidation in creek waters of tropical, seawater-dominated mangroves prevents 10 to 33% of the CH_4 outgassing. Large tidal ranges, deeper waters, high porewater exchange, and high organic carbon burial are associated with high oxidation rates in surface waters and low oxidation in porewater. Overall, porewater oxidation plays a major role regulating CH_4 emissions.

Our global upscaling revealed that CH_4 emissions from seawater-dominated mangroves were 0.010 Tg CH_4 yr^{-1} (or 1.02 Tg CO_2 yr^{-1} as CO_2e, using $SGWP_{20}$), with 60% of emissions originating from the water-atmosphere interface (Fig. 4; Extended Data Fig. 7; Supplementary Information Table S8). These emissions resulted in a relatively small offset of only 7% to sediment organic carbon burial. CH_4 emissions from freshwater-dominated mangroves were on average 14 times higher than seawater-dominated mangroves at 0.146 Tg CH_4 yr^{-1} (or 14.09 Tg CO_2 yr^{-1} as CO_2e, $SGWP_{20}$) with a similar contribution from sediment-atmosphere (54%) and water-atmosphere (46%) emissions. Freshwater-influenced mangroves could thus offset 27% of mangrove organic carbon burial. However, a large portion of that methane likely originates from upstream freshwater sources (Figure 1A). Indeed, a global compilation demonstrated that aquatic CH_4 emissions are 3 to 4-fold higher from rivers than mangroves[31]. Using the median fluxes for the entire dataset (still biased towards freshwater), the total global mangrove methane emissions are 0.068 Tg CH_4 yr^{-1} (or 6.54 Tg CO_2 yr^{-1} as CO_2e, $SGWP_{20}$), giving an offset of 15% which is lower than previous estimates of ~20%[14] (Fig. 4). Earlier global estimates used Global Warming Potential (GWP) metrics rather than the Sustained-Flux Global Warming Potential (SGWP) used here. The SGWP is generally larger and considered more realistic than the GWP for the comparison of the radiative forcing of different greenhouse gas emissions of natural ecosystems[15]. Therefore, accounting for seawater-dominated mangroves revealed that CH_4 emissions are a smaller offset to organic carbon burial in mangroves.

Organic carbon burial and CH_4 emissions rates can vary significantly between 3 to 4 orders of magnitude in mangroves[31,64]. Thus, local rates of carbon burial and CH_4 emissions should be compared. Unfortunately, concomitant data on carbon burial and CH_4 emissions remain scarce. Organic carbon burial depends on sedimentary (terrigenous or carbonate-dominant) and geomorphic (delta, estuaries, lagoons, open coasts) conditions[64]. We reveal that mangrove typologies and climates also influence CH_4 emissions. Tropical mangroves systems that account for ~85% of the world's mangrove area have the lowest offsets in both freshwater-influenced and seawater-dominated conditions. Therefore, our inclusion of distinct climates, typologies and the full latitudinal range offers a refined global mangrove CH_4 budget that decreases previously-estimated global offsets.

Our findings of higher ratios of CH_4 to CO_2 emissions in freshwater- than seawater-dominated pristine mangroves have implications for carbon budgets. Furthermore, pristine seawater-dominated mangroves can be a sink for N_2O[60]. CH_4 and N_2O are powerful greenhouse gases, so the conservation and restoration of mangroves should aim not only to enhance carbon burial, but also prevent greenhouse gas emissions to the atmosphere. We reveal much lower CH_4 offsets to carbon burial than previously thought. Preserving and restoring blue carbon ecosystems can partially contribute to the global efforts to sequester CO_2 from the atmosphere and prevent additional emissions. The lower

methane emissions revealed in our investigation enhance the perceived climate benefits of mangrove ecosystem restoration. We highlight, however, that potential blue carbon ecosystem restoration could draw down an additional 841 (621–1,064) Tg CO_2e per year by 2030 amounting to ~3% of the actual global anthropogenic emissions[3]. Hence, blue carbon ecosystems play a small role in mitigating climate change on a global scale[18]. A significant reduction in anthropogenic greenhouse gas emissions remains as the top priority to minimize climate change.

Acknowledgements

Funding for field investigations and analytical instrumentation was provided by the Australian Research Council to IRS (LE120100156 and DE140101733). Some of the analysis and travel were funded by the Swedish Research Council to IRS (2020-00457). GA was supported by the French-Brazilian International research project VELITROP (CNRS, INEE). LCCJr thanks the Fundação Cearense de Apoio ao Desenvolvimento Científico e Tecnológico (FUNCAP, INT- 00159-00009.01.00/19) and the Post Graduate Program in Tropical Marine Sciences of the Federal University of Ceará (UFC-PRPPG) for a visiting researcher grant at the Marine Sciences Institute (LABOMAR). LCCJr also thanks the German Federal Ministry of Education and Research through the Project Carbostore, grant nr. 03F0875B, for the Postdoctoral Fellowship Grant. The symbols used in the Fig. 4 and in the Extended Data Fig.7 are a courtesy of the Integration and Application Network (IAN), University of Maryland Center for Environmental Science (ian.umces.edu/media-library).

Author contribution statement

LCCJr performed most of the data analysis, made tables and figures, and wrote the first draft with support from IRS, GA, and others. IRS designed, managed and obtained funding for the project. GA supported the interpretation of methane isotopic composition and calculation of oxidation rates. CJS was responsible for sediment analysis and carbon burial estimates. DT, JZS, CH and DM helped design the field campaign and performed field and laboratory work. DTM and JZS calculated methane emissions and drafted some of the methods section. YYY drafted the introduction and performed some of the literature review. All authors edited the manuscript and approved its submission.

Competing Interests Statement

The authors declare no competing interests.

Figure Legends/Captions (for main text figures)

Fig 1. Dissolved CH_4 concentrations and emissions in seawater-dominated and freshwater-influenced mangroves. A) Dissolved CH_4 concentrations is driven by salinity in mangrove tidal creeks. Compiled literature data[5,14,32,73] (blue crosses) had overall significant freshwater influence. Our new data in seawater-dominated mangrove creeks (red crosses) reveal much lower CH_4 concentrations and emissions. Each cross in the graph (blue or red) represents a single measurement. The error bars represent the mean ± SD in each tidal creek. The dashed line represents the 3rd order polynomial regression incorporating all data points (R^2=0.22; n=9122). B) Compiled data of CH_4 versus CO_2 aquatic emissions in mangrove creeks revealing different trends for freshwater-influenced (salinity < 30) and seawater-dominated (salinity > 30) mangroves (Extended Data Fig. 1)[74]. The lines represent linear regressions. The raw data are provided in the open data repository Figshare (https://doi.org/10.6084/m9.figshare.24204351).

Fig. 2. Site-specific CH_4 emissions and offsets to organic carbon burial in seawater-dominated, pristine mangroves. A) The methane offset to organic carbon burial in mangroves. The dotted black line represents the previous global average based mostly on freshwater-dominated mangroves[14]. Details of offset calculation appear in Methods. B) The relationship between mean aquatic CH_4 emissions and mean organic carbon burial in seawater-dominated, pristine mangrove sediments spanning a latitudinal gradient. The error bars represent the standard deviation. Notice that the size of some data points in the graphs surpasses the standard deviation bars.

Fig. 3. Large CH_4 oxidation in mangroves revealed by $\delta^{13}C$-CH_4. (A) The comparison between mean $\delta^{13}C$-CH_4 signatures observed in mangrove porewater and those calculated from expected conservative in mangrove creek waters. The line represents a ratio of 1:1. (B) The relationship between mean $\delta^{13}C$-CH_4 signatures in porewater and mean rates of sediment OC burial. The trend line is a linear regression ($p < 0.05$). (C) The relationship between mean porewater exchange[67] and mean $\delta^{13}C$-CH_4 porewater signatures. The trendline is a linear regression ($p < 0.005$). (D) The fraction of CH_4 oxidation in the tidal creeks versus CH_4 concentrations. The results represent the mean ± SD of the two isotope fractionation models. The curve represents a two-phase association nonlinear regression that was fitted, incorporating all available data points (R^2=0.87; n=199). Details on the approach appear in Methods. All error bars represent mean ± SD. The size of some data points exceed standard deviation bars.

Fig. 4. Global upscaling of annual CH_4 emissions and organic carbon burial in sediments. Median (interquartile range) rates of CH_4 emissions and organic carbon burial in global mangroves were also calculated for seawater-dominated and freshwater-influenced ecosystem (Extended Data Fig. 7). Global mangroves were assumed to be inundated 50% of the time (water-atmosphere flux) and exposed 50% of the time. Plant-mediated CH_4 emissions were not included in the global upscaling due to lack of data and CH_4 ebullition was considered negligible. The fluxes were extracted from recent global compilations of mangrove CH_4 emissions[31] and organic carbon burial in mangrove sediments[64], and complemented by our observations. Fig. 7 in the Extended Data contrasts global budgets for seawater-dominated and freshwater-influenced mangroves.

References

1. McLeod, E. *et al.* A blueprint for blue carbon: Toward an improved understanding of the role of vegetated coastal habitats in sequestering CO2. *Front. Ecol. Environ.* **9**, 552–560 (2011).

2. Serrano, O. *et al.* Australian vegetated coastal ecosystems as global hotspots for climate change mitigation. *Nat. Commun.* **10**, 4313 (2019).

3. Macreadie, P. I. *et al.* Blue carbon as a natural climate solution. *Nat. Rev. Earth Environ.* **2**, 826–839 (2021).

4. Bouillon, S. *et al.* Mangrove production and carbon sinks: a revision of global budget estimates. *Glob. Biogeochem. Cy.* **22**, (2008).

5. Santos, I. R., Maher, D. T., Larkin, R., Webb, J. R. & Sanders, C. J. Carbon outwelling and outgassing vs. burial in an estuarine tidal creek surrounded by mangrove and saltmarsh wetlands. *Limnol. Oceanogr.* **64**, 996–1013 (2019).

6. Maher, D. T., Santos, I. R., Golsby-Smith, L., Gleeson, J. & Eyre, B. D. Groundwater-derived dissolved inorganic and organic carbon exports from a mangrove tidal creek: The missing mangrove carbon sink? *Limnol. Oceanogr.* **58**, 475–488 (2013).

7. Reithmaier, G. M. S. *et al.* Carbonate chemistry and carbon sequestration driven by inorganic carbon outwelling from mangroves and saltmarshes. *Nat. Commun.* **14**, 8196 (2023).

8. Rosentreter, J. A., Maher, D. T., Erler, D. V., Murray, R. & Eyre, B. D. Seasonal and temporal CO2dynamics in three tropical mangrove creeks – A revision of global mangrove CO2emissions. *Geochim. Cosmochim. Acta* **222**, 729–745 (2018).

9. Wang, F. *et al.* Global blue carbon accumulation in tidal wetlands increases with climate change. *Natl. Sci. Rev.* **8**, (2021).

10. Saintilan, N., Rogers, K., Mazumder, D. & Woodroffe, C. Allochthonous and autochthonous contributions to carbon accumulation and carbon store in southeastern Australian coastal wetlands. *Estuar. Coast. Shelf Sci.* **128**, 84–92 (2013).

11. Kristensen, E., Bouillon, S., Dittmar, T. & Marchand, C. Organic carbon dynamics in mangrove ecosystems: A review. *Aquat. Bot.* **89**, 201–219 (2008).

12. Barnes, J. *et al.* Tidal dynamics and rainfall control N2O and CH4 emissions from a pristine mangrove creek. *Geophys. Res. Lett.* **33**, 4–9 (2006).

13. Kristensen, E. *et al.* Emission of CO2 and CH4 to the atmosphere by sediments and open waters in two Tanzanian mangrove forests. *Mar. Ecol. Prog. Ser.* **370**, 53–67 (2008).

14. Rosentreter, J. A., Maher, D. T., Erler, D. V., Murray, R. H. & Eyre, B. D. Methane emissions partially offset "blue carbon" burial in mangroves. *Sci. Adv.* **4**, (2018).

15. Neubauer, S. C. & Megonigal, J. P. Moving Beyond Global Warming Potentials to Quantify the Climatic Role of Ecosystems. *Ecosystems* **18**, 1000–1013 (2015).

16. Al-Haj, A. N. & Fulweiler, R. W. A synthesis of methane emissions from shallow vegetated coastal ecosystems. *Glob. Chang. Biol.* **26**, 2988–3005 (2020).

17. Rosentreter, J. A. & Williamson, P. Concerns and uncertainties relating to methane emissions synthesis for vegetated coastal ecosystems. *Glob. Chang. Biol.* **26**, 5351–5352 (2020).

18. Williamson, P. & Gattuso, J.-P. Carbon Removal Using Coastal Blue Carbon Ecosystems Is Uncertain and Unreliable, With Questionable Climatic Cost-Effectiveness . *Frontiers in Climate* vol. 4 at https://www.frontiersin.org/articles/10.3389/fclim.2022.853666 (2022).

19. Liu, J. *et al.* Methane emissions reduce the radiative cooling effect of a subtropical estuarine mangrove wetland by half. *Glob. Chang. Biol.* **26**, 4998–5016 (2020).

20. Borges, A. V. & Abril, G. *Carbon Dioxide and Methane Dynamics in Estuaries. Treatise on Estuarine and Coastal Science* vol. 5 (2011).

21. Bouillon, S. *et al.* Importance of intertidal intertidal sediment processes and porewater exchange on the water column biogeochemistry in a pristine mangrove creek (Ras Dege, Tanzania). *Biogeosciences* **4**, 311–322 (2007).

22. Call, M. *et al.* Spatial and temporal variability of carbon dioxide and methane fluxes over semi-diurnal and spring–neap–spring timescales in a mangrove creek. *Geochim. Cosmochim. Acta* **150**, 211–225 (2015).

23. King, G. M. Ecological Aspects of Methane Oxidation, a Key Determinant of Global Methane Dynamics BT - Advances in Microbial Ecology. in (ed. Marshall, K. C.) 431–468 (Springer US, 1992). doi:10.1007/978-1-4684-7609-5_9.

24. Van Der Nat, F. J. W. A., De Brouwer, J. F. C., Middelburg, J. J. & Laanbroek, H. J. Spatial distribution and inhibition by ammonium of methane oxidation in intertidal freshwater marshes. *Appl. Environ. Microbiol.* **63**, 4734–4740 (1997).

25. Sánchez-Carrillo, S. *et al.* Methane production and oxidation in mangrove soils assessed by stable isotope mass balances. *Water (Switzerland)* **13**, 1–22 (2021).

26. Whiticar, M. J. *The Biogeochemical Methane Cycle*. *Hydrocarbons, Oils and Lipids: Diversity, Origin, Chemistry and Fate* (2020). doi:10.1007/978-3-319-54529-5_5-1.

27. Whiticar, M. J. Carbon and hydrogen isotope systematics of bacterial formation and oxidation of methane. *Chem. Geol.* **161**, 291–314 (1999).

28. Bastviken, D., Ejlertsson, J. & Tranvik, L. Measurement of Methane Oxidation in Lakes: A Comparison of Methods. *Environ. Sci. Technol.* **36**, 3354–3361 (2002).

29. Call, M. *et al.* High pore-water derived CO 2 and CH 4 emissions from a macro-tidal mangrove creek in the Amazon region. *Geochim. Cosmochim. Acta* **247**, 106–120 (2019).

30. Rosentreter, J. A., Maher, D. T., Erler, D. V, Murray, R. & Eyre, B. D. Factors controlling seasonal CO2 and CH4 emissions in three tropical mangrove-dominated estuaries in Australia. *Estuar. Coast. Shelf Sci.* **215**, 69–82 (2018).

31. Rosentreter, J. A. *et al.* Half of global methane emissions come from highly variable aquatic ecosystem sources. *Nat. Geosci.* **14**, 225–230 (2021).

32. Borges, A. V, Abril, G. & Bouillon, S. Carbon dynamics and CO2 and CH4 outgassing in the Mekong delta. *Biogeosciences* **15**, 1093–1114 (2018).

33. Alongi, D. M. Carbon cycling in the world's mangrove ecosystems revisited: Significance of non-steady state diagenesis and subsurface linkages between the forest floor and the coastal ocean. *Forests* **11**, 1–17 (2020).

34. Chen, G. C. *et al.* Rich soil carbon and nitrogen but low atmospheric greenhouse gas fluxes from North Sulawesi mangrove swamps in Indonesia. *Sci. Total Environ.* **487**, 91–96 (2014).

35. Barroso, G. C. *et al.* Linking eutrophication to carbon dioxide and methane emissions from exposed mangrove soils along an urban gradient. *Sci. Total Environ.* **850**, 157988 (2022).

36. Sadat-Noori, M., Maher, D. T. & Santos, I. R. Groundwater Discharge as a Source of Dissolved Carbon and Greenhouse Gases in a Subtropical Estuary. *Estuaries and Coasts* **39**, 639–656 (2016).

37. Martens, C. S., Albert, D. B. & Alperin, M. J. Biogeochemical processes controlling methane in gassy coastal sediments—Part 1. A model coupling organic matter flux to gas production, oxidation and transport. *Cont. Shelf Res.* **18**, 1741–1770 (1998).

38. Gonsalves, M.-J., Fernandes, C. E. G., Fernandes, S. O., Kirchman, D. L. & Bharathi, P. A. L. Effects of composition of labile organic matter on biogenic production of methane in the coastal sediments of the Arabian Sea. *Environ. Monit. Assess.* **182**, 385–395 (2011).

39. Poffenbarger, H. J., Needelman, B. A. & Megonigal, J. P. Salinity Influence on Methane Emissions from Tidal Marshes. *Wetlands* **31**, 831–842 (2011).

40. Sea, M. A., Garcias-Bonet, N., Saderne, V. & Duarte, C. M. Carbon dioxide and methane fluxes at the air–sea interface of Red Sea mangroves. *Biogeosciences* **15**, 5365–5375 (2018).

41. Jeffrey, L. C. *et al.* Are methane emissions from mangrove stems a cryptic carbon loss pathway? Insights from a catastrophic forest mortality. *New Phytol.* **224**, 146–154 (2019).

42. Gao, C.-H. *et al.* Source or sink? A study on the methane flux from mangroves stems in Zhangjiang estuary, southeast coast of China. *Sci. Total Environ.* **788**, 147782 (2021).

43. Zhang, C. *et al.* Massive methane emission from tree stems and pneumatophores in a subtropical mangrove wetland. *Plant Soil* **473**, 489–505 (2022).

44. Krithika, K., Purvaja, R. & Ramesh, R. Fluxes of methane and nitrous oxide from an Indian mangrove. **94**, (2008).

45. Padhy, S. R. *et al.* Seasonal fluctuation in three mode of greenhouse gases emission in relation to soil labile carbon pools in degraded mangrove, Sundarban, India. *Sci. Total Environ.* **705**, 135909 (2020).

46. Chuang, P. C. *et al.* Methane fluxes from tropical coastal lagoons surrounded by mangroves, Yucatán, Mexico. *J. Geophys. Res. Biogeosciences* **122**, 1156–1174 (2017).

47. Li, C.-H., Zhou, H.-W., Wong, Y.-S. & Tam, N. F.-Y. Vertical distribution and anaerobic biodegradation of polycyclic aromatic hydrocarbons in mangrove sediments in Hong Kong, South China. *Sci. Total Environ.* **407**, 5772–5779 (2009).

48. Middelburg, J. J. *et al.* Organic matter mineralization in intertidal sediments along an estuarine gradient. *Mar. Ecol. Prog. Ser.* **132**, 157–168 (1996).

49. Chanton, J. P., Martens, C. S. & Kelley, C. A. Gas transport from methane-saturated, tidal freshwater and wetland sediments. *Limnol. Oceanogr.* **34**, 807–819 (1989).

50. McGenity, T. J. & Sorokin, D. Y. Methanogens and Methanogenesis in Hypersaline Environments BT - Biogenesis of Hydrocarbons. in (eds. Stams, A. J. M. & Sousa, D.) 1–27 (Springer International Publishing, 2018). doi:10.1007/978-3-319-53114-4_12-1.

51. Boetius, A. *et al.* A marine microbial consortium apparently mediating anaerobic oxidation of methane. *Nature* **407**, 623–626 (2000).

52. Reeburgh, W. S. Oceanic methane biogeochemistry. *Chem. Rev.* **107**, 486–513 (2007).

53. Marchand, C., David, F., Jacotot, A., Leopold, A. & Ouyang, X. Chapter 3 - CO2 and CH4 emissions from coastal wetland soils. in *Estuarine and Coastal Sciences Series* (eds. Ouyang, X., Lee, S. Y., Lai, D. Y. F. & Marchand, C. B. T.-C. M. in C. W.) vol. 2 55–91 (Elsevier, 2022).

54. Weston, N. B., Dixon, R. E. & Joye, S. B. Ramifications of increased salinity in tidal freshwater sediments: Geochemistry and microbial pathways of organic matter mineralization. *J. Geophys. Res. Biogeosciences* **111**, (2006).

55. Martens, C. S. & Berner, R. A. Methane Production in the Interstitial Waters of Sulfate-Depleted Marine Sediments. *Science (80-.).* **185**, 1167–1169 (1974).

56. Bartlett, K. B., Bartlett, D. S., Harriss, R. C. & Sebacher, D. I. Methane emissions along a salt marsh salinity gradient. *Biogeochemistry* **4**, 183–202 (1987).

57. Chambers, L. G., Reddy, K. R. & Osborne, T. Z. Short-Term Response of Carbon Cycling to Salinity Pulses in a Freshwater Wetland. *Soil Sci. Soc. Am. J.* **75**, 2000–2007 (2011).

58. Maher, D. T., Cowley, K., Santos, I. R., Macklin, P. & Eyre, B. D. Methane and carbon dioxide dynamics in a subtropical estuary over a diel cycle: Insights from automated in situ radioactive and stable isotope measurements. *Mar. Chem.* **168**, 69–79 (2015).

59. Yau, Y. Y. Y. *et al.* Alkalinity export to the ocean is a major carbon sequestration mechanism in a macrotidal saltmarsh. *Limnol. Oceanogr.* (2022) doi:10.1002/lno.12155.

60. Maher, D. T., Sippo, J. Z., Tait, D. R., Holloway, C. & Santos, I. R. Pristine mangrove creek waters are a sink of nitrous oxide. *Sci. Rep.* **6**, 1–8 (2016).

61. Twilley, R. R., Chen, R. H. & Hargis, T. Carbon sinks in mangroves and their implications to carbon budget of tropical coastal ecosystems. *Water. Air. Soil Pollut.* **64**, 265–288 (1992).

62. Sanders, C. J. *et al.* Are global mangrove carbon stocks driven by rainfall? *J. Geophys. Res. G Biogeosciences* **121**, 2600–2609 (2016).

63. Abril, G. & Iversen, N. Methane dynamics in a shallow non-tidal estuary (Randers Fjord,

Denmark). *Mar. Ecol. Prog. Ser.* **230**, 171–181 (2002).

64. Breithaupt, J. L. & Steinmuller, H. E. Refining the Global Estimate of Mangrove Carbon Burial Rates Using Sedimentary and Geomorphic Settings. *Geophys. Res. Lett.* **49**, e2022GL100177 (2022).

65. Worthington, T. A. *et al.* A global biophysical typology of mangroves and its relevance for ecosystem structure and deforestation. *Sci. Rep.* **10**, 1–12 (2020).

66. Iversen, N. Methane Oxidation in Coastal Marine Environments BT - Microbiology of Atmospheric Trace Gases. in (eds. Murrell, J. C. & Kelly, D. P.) 51–68 (Springer Berlin Heidelberg, 1996).

67. Tait, D. R., Maher, D. T., Macklin, P. A. & Santos, I. R. Mangrove pore water exchange across a latitudinal gradient. *Geophys. Res. Lett.* **43**, 3334–3341 (2016).

68. Lugo, A. E. & Snedaker, S. C. The Ecology of Mangroves. *Annu. Rev. Ecol. Syst.* **5**, 39–64 (1974).

69. Reithmaier, G. M. S., Ho, D. T., Johnston, S. G. & Maher, D. T. Mangroves as a Source of Greenhouse Gases to the Atmosphere and Alkalinity and Dissolved Carbon to the Coastal Ocean: A Case Study From the Everglades National Park, Florida. *J. Geophys. Res. Biogeosciences* **125**, 1–16 (2020).

70. Dutta, M. K., Mukherjee, R., Jana, T. K. & Mukhopadhyay, S. K. Biogeochemical dynamics of exogenous methane in an estuary associated to a mangrove biosphere; The Sundarbans, NE coast of India. *Mar. Chem.* **170**, 1–10 (2015).

71. Dutta, M. K., Bianchi, T. S. & Mukhopadhyay, S. K. Mangrove methane biogeochemistry in the Indian Sundarbans: A proposed budget. *Front. Mar. Sci.* **4**, 1–15 (2017).

72. Das, S., Ganguly, D., Chakraborty, S., Mukherjee, A. & Kumar De, T. Methane flux dynamics in relation to methanogenic and methanotrophic populations in the soil of Indian Sundarban mangroves. *Mar. Ecol.* **39**, e12493 (2018).

73. Linto, N. *et al.* Carbon Dioxide and Methane Emissions from Mangrove-Associated Waters of the Andaman Islands, Bay of Bengal. *Estuaries and Coasts* **37**, 381–398 (2014).

74. Giri, C. *et al.* Status and distribution of mangrove forests of the world using earth observation satellite data. *Glob. Ecol. Biogeogr.* **20**, 154–159 (2011).

Methods

Study sites

This study combines new observations from six seawater-dominated mangroves across a latitudinal gradient (Extended Data Figs. 1-5; Supplementary Information Table S1) with literature data (Supplementary Information Table S8) to resolve the contribution of methane emissions as an offset to mangrove carbon sequestration. Field studies were undertaken in pristine mangrove tidal creeks on the northern, eastern and southern Australian coastlines over a latitudinal range covering all climatic regions relevant to mangroves. Field study sites had low-lying catchments (< 5.5 m) and had minimal freshwater inputs with no riverine water sources. Site characteristics followed a latitudinal trend, with an overall increased average rainfall, temperature, and mangrove diversity at lower latitudes (Supplementary Information Table S1). Tidal amplitude ranged from a macrotidal system in Darwin (4.2 m), mesotidal systems at Hinchinbrook Island (2.4 m) and Seventeen Seventy (2.4 m), and microtidal systems at Moreton Bay (1.5 m), Newcastle (1.1 m) and Barwon Heads (0.7 m). This work expands on studies at the same locations which examined porewater exchange[67], alkalinity dynamics[75],

nitrous oxide fluxes[60], trace metal fluxes[76], carbon stock estimates[62] and exchangeable dissolved organic carbon[77]. All the CH_4 concentration and stable isotopes as well as sediment carbon burial datasets are original.

Surface water and porewater observations

Dissolved CO_2 and CH_4 concentrations and $\delta^{13}C$ isotopes were measured near the mouth of mangrove tidal creeks at the six field sites (Extended Data Fig. 1). The continuous, real-time measurements of dissolved CH_4 lasted between a minimum of ~101 hours (~4.2 days, Melbourne mangrove) to a maximum deployment of ~409 hours (~17 days, Moreton Bay mangrove). This is an unprecedented sampling effort as the large majority of studies investigating dissolved CH_4 concentrations and fluxes only sampled over semi-diurnal (~13 hours) or diel (~24 hours) time scales.

High-precision concentrations and isotopes were measured using a cavity ring-down spectrometer (CRDS; Picarro G2201-I)[78,79]. Water column CH_4 and isotopes were measured by continuously pumping water from a depth of ~25 cm via a submersible pump (Rule 500 GPH) at ~2.8 L into two connected showerhead gas equilibration devices[80,81]. The first equilibrator, which is vented to the atmosphere via 2 m of coiled gas tight tubing (Bev-A-Line® IV; (1/8" ID, 1/4" OD), prevents the build-up of pressure in the main equilibrator, thus reducing analytic uncertainties[81]. Equilibrated headspace air from the second equilibrator was then pumped through gas-tight tubing into a desiccant cannister (Drierite) and then into the CRDS. Concentrations and isotopes of dissolved gases were measured at one-second intervals and then averaged over one-minute intervals. The response time for equilibration using the system was approximately 30 minutes[79] which was accounted for in presenting the data. Instrument precision for CH_4 concentrations given by the manufacturer is 60 ppb + 0.05%. The CRDS was calibrated using 0, 400 and 2000 ppb gas standards (Air Liquide, Australia), both before and after measurements at each site. Instrument drift was < 1% between calibrations.

High-resolution measurements of water depth and current velocity were taken at the same sites using an acoustic doppler current profiler (SonTek Argonaut), with measurements taken at one second intervals and averaged over one-minute intervals. Additional water parameters (salinity, temperature and luminescent dissolved oxygen) were measured at one-minute intervals using a multi-parameter water quality sonde (Hydrolab DS 5X).

Dissolved CH_4 concentrations were calculated from pCH_4 using the temperature and salinity dependant solubility equations of Wiesenburg and Guinasso (1979)[82]. Emissions of CH_4 (FCH_4) from surface waters were calculated according to:

$$FCH_4 = k\alpha(\Delta pCH_4) \quad \text{(Eq. 1)}$$

where k is the transfer velocity, α is the temperature and salinity solubility[82] and ΔpCH_4 is the difference between atmospheric pCH_4 and water column pCH_4. The water pCH_4 was measured with the continuous measurement system described above. The atmospheric pCH_4 was determined from observations (at least three measurements for each day, between the aquatic measurements). The gas transfer velocity was calculated using four different empirical relationships[83–86] in order to provide ranges of estimations. The air-water CH_4 exchanges (diffusive fluxes) were calculated over two complete tidal cycles (integrating ~24 hours and 50 minutes), and averaged daily for the entire period[5,6]. The time series deployment ranged between a minimum of 101 hours (~4-day period; Melbourne mangrove) to a maximum of 409 hours (~17-day period; Moreton Bay mangrove). In each catchment area, a digital elevation model (DEM) was used to create a delineated catchment using LiDAR data (1 m resolution with ± 0.2 m elevation accuracy). Catchment water volume was calculated for each site at ten-minute intervals using the DEM and ARC GIS Hydrology toolbox[6,67,75].

Considering all six mangroves, the maximal inundated area during flooded tide was >80%, on average[67].

The groundwater sampling occurred simultaneously with time series deployment in surface waters. Groundwater pCH_4 and $\delta^{13}C\text{-}CH_4$ were measured via headspace equilibration. Briefly, bores were dug at 10-12 sites along each mangrove creek at the low tide mark. Water was pumped using a peristaltic pump into opaque 250 ml bottles, from which samples were extracted using the discrete headspace method[87]. Concentrations were calculated using the methods described by Hope et al. (1995)[88] exchanging the Henry's Law constant for that of CH_4. An isotope mass balance was used to estimate the original $\delta^{13}C\text{-}CH_4$ of groundwater by accounting for the ambient air headspace in the bottles at the start of the equilibration. No porewater data were available for the Moreton Bay site (27°S).

Sedimentary organic carbon analysis and rates of organic carbon burial

At each of the study sites, sediment cores were extracted from near the mangrove fringe (lower tidal), and well within the forest (upper tidal) using a Russian Peat Auger at low tide. Each sediment core was sectioned at 2-cm intervals from the surface to a 10 cm depth, and at 5-cm intervals until a 50 cm depth. The dry bulk density (DBD) (g cm^{-3}) for each interval was determined as the dry sediment weight (g) divided by the sediment core interval initial volume (cm^3). A homogenized portion of each sediment interval was acidified to remove carbonate material, then dried and ground to powder for organic carbon (OC) analyses, using a Flash Elemental Analyser coupled to a Thermo Fisher Delta V IRMS (isotope ratio mass spectrometer). The analytical precision of these analyses was 0.1%.

The procedures for $^{239+240}Pu$ measurements followed well established approaches developed by Ketterer et al.[89] and adopted for coastal wetland sediments[5]. The detection limits for this procedure were determined through the analyses of powdered rock samples devoid of detectable Pu and used as negative controls. Aliquots of a U.S. Department of Energy control sample (Mixed Analyte Performance Evaluation Program (MAPEP; 01-S8) were found to be very similar to the experimental results found herein (± 2%). For a sample of nominal 10 g mass, the detection limit was established as 0.01 Bg kg^{-1} of $^{239+240}Pu$.

In the upper and lower tidal area of each of the six sites, two sediment cores were taken for $^{239+240}Pu$ dating, as in previous studies[90]. This dating model is based on the fact that $^{239+240}Pu$-activities are anthropogenic in origin and were not introduced into the environment before the 1950's. Therefore, material below the first occurrence of $^{239+240}Pu$ activity represents pre-bomb deposited sediments (Supplementary Information Fig. S7). This appropriately affixes an upper limit on the sediment accretion at each study site. The carbon burial estimates were based on the sediment accretion, dry bulk density (DBD) and carbon content of each sediment core, with 144 samples in total (Supplementary Information Fig. S7). The carbon burial results highlight that mangroves bury carbon at different rates along coastal settings characterized by different climates, sediment types, tidal amplitudes and by variations in geomorphologies, as has also been noted in global estimates[9].

CO_2 equivalent emissions of CH_4 (CO_2e) and offset calculations

To compare the radiative forcing of greenhouse gases we applied the Sustained-Flux Global Warming Potentials (SGWPs)[91] instead of the Global Warming Potential (GWP). Although the measured CH_4 emissions and carbon burial rates operate over very different timescales, we assumed that CH_4 production has been in steady state over the longer time frame of carbon burial[14]. The SGWPs of CH_4 are 96 and 45 for time horizons of 20 and 100 years, respectively. Since CH_4 has a short lifetime in the atmosphere (9.1 ± 0.9 years), we choose the time horizon of 20 years ($SGWP_{20}$). For comparison

purposes we also present the $SGWP_{100}$ time horizon. The CO_2 equivalent emissions of CH_4 ($FCH_4(CO_{2eq})$) were calculated as:

$$FCH_4(CO_2e) = FCH_{4emission} * SGWP \quad \text{(Eq. 2)}$$

Where $FCH_{4emission}$ is the mangrove aquatic emission of CH_4 (Mg CH_4 yr^{-1}); SGWP is 96 and 45 for time horizons of 20 and 100 years, respectively.

The CH_4 offset relative to carbon burial was calculated using modified calculations from Rosentreter et al.[14] where the authors compared global CH_4 emissions to global carbon burial. Here, we compared local rates of aquatic emissions of CH_4 with local rates of organic carbon burial to obtain a more appropriate offset estimate. The aquatic emissions of CH_4 as CO_2e for the time horizon of 20 years ($SGWP_{20}$) were compared with carbon burial rate as CO_2e, in each mangrove. For comparison purposes, we used the conversion factor of 3.6667 (44/12) to convert the organic carbon burial (Mg C yr^{-1}) to CO_2e (Mg CO_2 yr^{-1}).

Methane oxidation in surface waters of tidal creeks

The calculation of CH_4 oxidation was based on the ^{13}C fractionation considering that $\delta^{13}C$-CH_4 is gradually elevated during CH_4 oxidation[26,28]. Here, we modified a method originally applied to lakes[28]. Methane oxidation was calculated in surface waters based on CH_4 concentrations and $\delta^{13}C$-CH_4 data and ^{13}C fractionation. We first estimate the $\delta^{13}C$ signature of the CH_4 added by methanogenesis at each site. The $\delta^{13}C$ of the added CH_4 was calculated in two ways: (1) By considering a simple conservative mixing between two sources (porewater and tidal creek surface water) and (2) using keeling plots[92]. The two methods gave consistent results, and we considered the source signature as the average between these two values. Two models of isotope fractionation for open systems at steady state[93,94] were then applied:

$$f_{open} = (\delta s - \delta p) / ((\alpha - 1) * 1000) \quad \text{(Eq. 3)}$$

$$f_{open} = (\delta p - \delta s) / ((\delta s + 1000) ((1/\alpha) - 1)) \quad \text{(Eq. 4)}$$

where f_{open} is the fraction of the porewater CH_4 entering the tidal creek water that becomes oxidized. δs and δp are the $\delta^{13}C$ values measured in the tidal creek and in the porewater, respectively. Both models yielded comparable results within 10%, and the f_{open} values are presented as averages between the two models. We compared the measured $\delta^{13}C$-CH_4 values in porewaters (Supplementary Information Table S3) with the added $\delta^{13}C$-CH_4 calculated in each tidal creek (referenced to as a "conservative" $\delta^{13}C$-CH_4 values). The measured $\delta^{13}C$-CH_4 of porewater in the two mangroves where the observed and conservative $\delta^{13}C$-CH_4 were similar and close to the 1:1 line was used to calculate the oxidation rates in surface water of tidal creeks (Fig. 3A). Our method of calculating CH_4 oxidation in the tidal creek (surface water) is based on the comparison between the $\delta^{13}C$-CH_4 values observed in the porewater end-member and $\delta^{13}C$-CH_4 in surface waters. From the five mangrove sites where we sampled the porewater end-member, the averaged $\delta^{13}C$-CH_4 values matched that predicted through Keeling plots in two sites (the two tropical ecosystems; Darwin and Hinchbrook), suggesting no significant oxidation in the porewater. The Keeling plot approach is based upon mass conservation considerations during the exchange of carbon between two reservoirs[95]. In the three other mangroves, the $\delta^{13}C$-CH_4 from the keeling plot was much lighter than that measured in the porewater (Fig. 3A) revealing the occurrence of methane oxidation in porewater. However, CH_4 oxidation rates in the mangrove porewaters could not be calculated because these difference were not only due to oxidation, but also to the fact that tidal exchange mobilized porewater from different depths with different CH_4 concentrations and isotopic signatures. The isotope fractionation factor α can be variable in marine habitats (1.012-1.043[25,96]). We used the values of 1.025 and 1.033 found in wetlands[97]. By multiplying the fraction of CH_4 oxidation

by the aquatic CH_4 emissions we calculated the rates of CH_4 oxidation in creek surface waters by considering that the emitted CH_4 represents the fraction escaping oxidation[28], as follows:

$$Mox_{tidalcreek} = f_{open} * FCH_4/(1 - f_{open}) \quad \text{(Eq. 5)}$$

Where $Mox_{tidalcreek}$ is the rate of CH_4 oxidation in the tidal creek, and FCH_4 is the aquatic emission of FCH_4.

Global Upscaling

We performed a global upscaling of CH_4 emissions with three scenarios: global freshwater-influenced mangroves (salinity < 30), global seawater-dominated mangroves (salinity > 30), global mangroves (freshwater-influenced and seawater-dominated mangroves), and compared to the rates of organic carbon burial in sediments. Median (and interquartile) values of CH_4 emissions and organic carbon burial were calculated separately for each data set: global seawater-dominated mangroves, global freshwater-influenced mangroves, and global mangroves.The freshwater-influenced mangroves were considered the "deltaic (54,972 km^2)" and "estuarine (37,411 km^2)" types, while the seawater-dominated mangroves were considered the "lagoonal (14,993 km^2)" and "open coasts (28,493 km^2)" according to the typology of Worthington[65]. We compiled data of the CH_4 fluxes provided in the latest global assessment of CH_4 emissions[31], which were complemented by our six seawater-dominated sites. We only included studies that present information about the interface of CH_4 emission (sediment-atmosphere, water-atmosphere) and salinity. The organic carbon burial data in mangrove sediments were taken from the last global compilation[64], and were also complemented by the results of our six seawater-dominated mangroves as well. This last global compilation also used the biophysical typology of Worthington (delta, estuary, lagoon, and open coast mangroves) to refine the global estimate of mangrove carbon burial. Therefore, we compared rates of CH_4 emissions and the rates of carbon burial for similar mangrove biophysical typologies. Mangrove ecosystems were considered being inundated 50% of the time (water-atmosphere flux) and exposed 50% of the time (sediment-atmosphere flux) in freshwater-influenced mangroves[14]. For seawater-dominated sites, the mangroves were considered being inundated 65% of the time (water-atmosphere flux) and exposed 35% of the time (sediment-atmosphere flux)[67]. The CO_2 equivalent emissions of CH_4 and offset calculations were calculated similarly as described in previous sections. We used median values instead of mean values due to the non-normal distribution of the data. Plant-mediated CH_4 emissions were not included in the global upscaling due to the very low data availability. Ebullition based water-atmosphere emission was considered negligible as in coastal sediments CH_4 ebullition is tightly coupled to the variation of the tidal height and occurs almost exclusively around low tide when hydrostatic pressure is minimal[20]. In the case of intertidal ecosystems like mangroves, ebullition potentially occurs during the sediment emersion period and is thus captured by static chambers and included in the sediment-atmosphere fluxes[48].

Data availability statement

The raw data sets of all new observations and literature compilation are available on Figshare (https://doi.org/10.6084/m9.figshare.24204351)[98].

Methods-only references

75. Sippo, J. Z., Maher, D. T., Tait, D. R., Holloway, C. & Santos, I. R. Are mangroves drivers or buffers of coastal acidification? Insights from alkalinity and dissolved inorganic carbon export estimates across a latitudinal transect. *Global Biogeochem. Cycles* **30**, 753–766 (2016).

731 76. Holloway, C. J. *et al.* Manganese and iron release from mangrove porewaters: A significant
732 component of oceanic budgets? *Mar. Chem.* **184**, 43–52 (2016).

733 77. Sippo, J. Z. *et al.* Mangrove outwelling is a significant source of oceanic exchangeable organic
734 carbon. *Limnol. Oceanogr. Lett.* **2**, 1–8 (2017).

735 78. Maher, D. T. *et al.* Novel use of cavity ring-down spectroscopy to investigate aquatic carbon
736 cycling from microbial to ecosystem scales. *Environ. Sci. Technol.* **47**, 12938–45 (2013).

737 79. Webb, J. R., Maher, D. T. & Santos, I. R. Automated, in situ measurements of dissolved CO 2
738 , CH 4 , and δ 13 C values using cavity enhanced laser absorption spectrometry: Comparing response
739 times of air-water equilibrators. *Limnol. Oceanogr. Methods* n/a-n/a (2016) doi:10.1002/lom3.10092.

740 80. Pierrot, D. *et al.* Recommendations for autonomous underway pCO2 measuring systems and
741 data-reduction routines. *Deep Sea Res. Part II Top. Stud. Oceanogr.* **56**, 512–522 (2009).

742 81. Santos, I. R., Maher, D. T. & Eyre, B. D. Coupling automated radon and carbon dioxide
743 measurements in coastal waters. *Environ. Sci. Technol.* **46**, 7685–91 (2012).

744 82. Wiesenburg, D. A. & Guinasso, N. L. Equilibrium solubilities of methane, carbon monoxide,
745 and hydrogen in water and sea water. *J. Chem. Eng. Data* **24**, 356–360 (1979).

746 83. Wanninkhof, R. Relationship Between Wind Speed and Gas Exchange. *J. Geophys. Res.* **97**,
747 7373–7382 (1992).

748 84. Raymond, P. a. & Cole, J. J. Gas Exchange in Rivers and Estuaries: Choosing a Gas Transfer
749 Velocity. *Estuaries* **24**, 312 (2001).

750 85. Borges, A. V., Delille, B., Schiettecatte, L., Talence, F.- & Frankignoulle, M. Gas transfer
751 velocities of CO 2 in three European estuaries (Randers Fjord ,. **49**, 1630–1641 (2004).

752 86. Ho, D. T., Ferrón, S., Engel, V. C., Larsen, L. G. & Barr, J. G. Air-water gas exchange and
753 CO 2 flux in a mangrove-dominated estuary. *Geophys. Res. Lett.* **41**, 108–113 (2014).

754 87. Gatland, J. R., Santos, I. R., Maher, D. T., Duncan, T. M. & Erler, D. V. Carbon dioxide and
755 methane emissions from an artificially drained coastal wetland during a flood: Implications for
756 wetland global warming potential. *J. Geophys. Res. Biogeosciences* **119**, 1698–1716 (2014).

757 88. Hope, D., Dawson, J. J. C., Cresser, M. S. & Billett, M. F. A method for measuring free CO2
758 in upland streamwater using headspace analysis. *J. Hydrol.* **166**, 1–14 (1995).

759 89. Ketterer, M. E., Hafer, K. M., Jones, V. J. & Appleby, P. G. Rapid dating of recent sediments
760 in Loch Ness: inductively coupled plasma mass spectrometric measurements of global fallout
761 plutonium. *Sci. Total Environ.* **322**, 221–229 (2004).

762 90. Sanders, C. J. *et al.* Elevated rates of organic carbon, nitrogen, and phosphorus accumulation
763 in a highly impacted mangrove wetland. *Geophys. Res. Lett.* **41**, 2475–2480 (2014).

764 91. Neubauer, S. C. & Megonigal, J. P. Correction to: Moving Beyond Global Warming Potentials
765 to Quantify the Climatic Role of Ecosystems. *Ecosystems* **22**, 1931–1932 (2019).

766 92. Abril, G. *et al.* Export of 13C-depleted dissolved inorganic carbon from a tidal forest
767 bordering the Amazon estuary. *Estuar. Coast. Shelf Sci.* **129**, 23–27 (2013).

768 93. Happell, J. D., Chanton, J. P. & Showers, W. S. The influence of methane oxidation on the
769 stable isotopic composition of methane emitted from Florida swamp forests. *Geochim. Cosmochim.*
770 *Acta* **58**, 4377–4388 (1994).

94. Tyler, S. C., Bilek, R. S., Sass, R. L. & Fisher, F. M. Methane oxidation and pathways of production in a Texas paddy field deduced from measurements of flux, δl3C, and δD of CH4. *Global Biogeochem. Cycles* **11**, 323–348 (1997).

95. Köhler, P., Fischer, H., Schmitt, J. & Munhoven, G. On the application and interpretation of Keeling plots in paleo climate research – deciphering δ^{13}C of atmospheric CO_2 measured in ice cores. *Biogeosciences* **3**, 539–556 (2006).

96. Holler, T. *et al.* Substantial 13C/12C and D/H fractionation during anaerobic oxidation of methane by marine consortia enriched in vitro. *Environ. Microbiol. Rep.* **1**, 370–376 (2009).

97. Ward, N. D. *et al.* Pathways for Methane Emissions and Oxidation that Influence the Net Carbon Balance of a Subtropical Cypress Swamp. *Front. Earth Sci.* **8**, 1–16 (2020).

98. Cotovicz, L.C. et al. Methane oxidation minimizes emissions and offsets to carbon burial in mangroves. Data sets. figshare. https://doi.org/10.6084/m9.figshare.24204351 (2023).

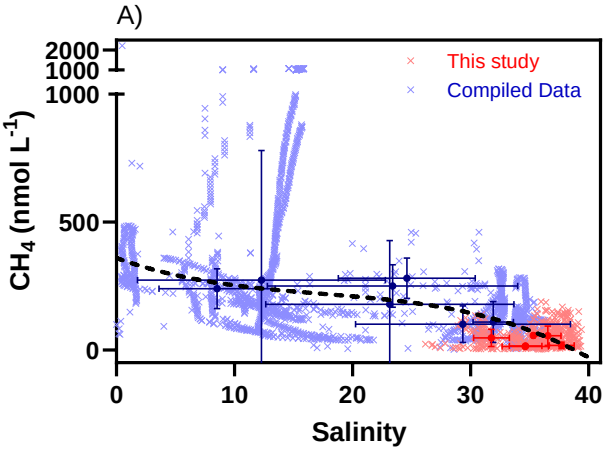
A)
2000
1000
1000
500
0
0
10
20
30
40
CH4 (nmol L-1)
Salinity
This study
Compiled Data

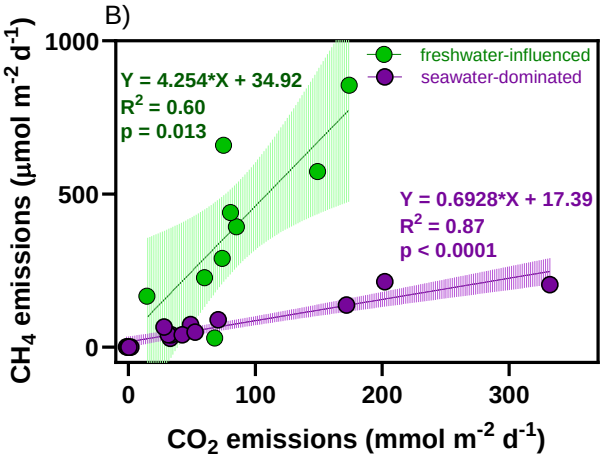
B)
1000
500
0
0
100
200
300
CH4 emissions (µmol m-2 d-1)
CO2 emissions (mmol m-2 d-1)
freshwater-influenced
seawater-dominated
Y = 4.254*X + 34.92
R2 = 0.60
p = 0.013
Y = 0.6928*X + 17.39
R2 = 0.87
p < 0.0001

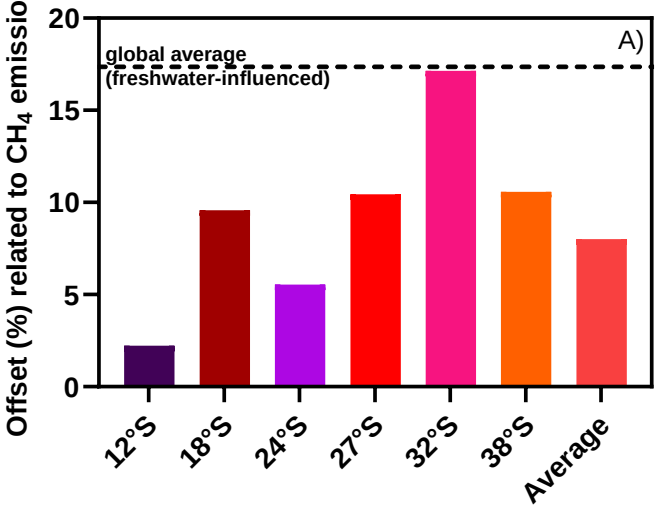
A)
global average
(freshwater-influenced)
Offset (%) related to CH4 emissions
20
15
10
5
0
12°S
18°S
24°S
27°S
32°S
38°S
Average

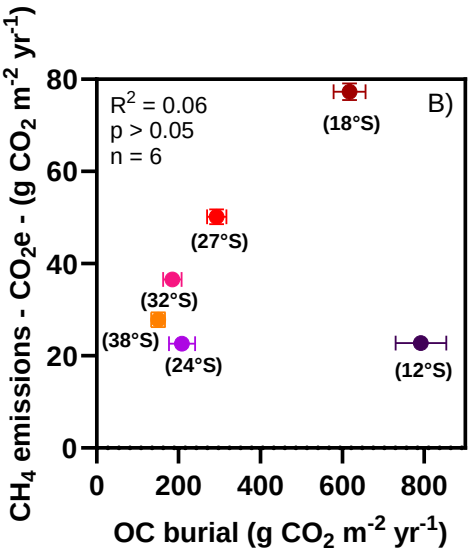
B)
R2 = 0.06
p > 0.05
n = 6
(18°S)
(27°S)
(32°S)
(38°S)
(24°S)
(12°S)
CH4 emissions - CO2e - (g CO2 m-2 yr-1)
OC burial (g CO2 m-2 yr-1)
80
60
40
20
0
0
200
400
600
800

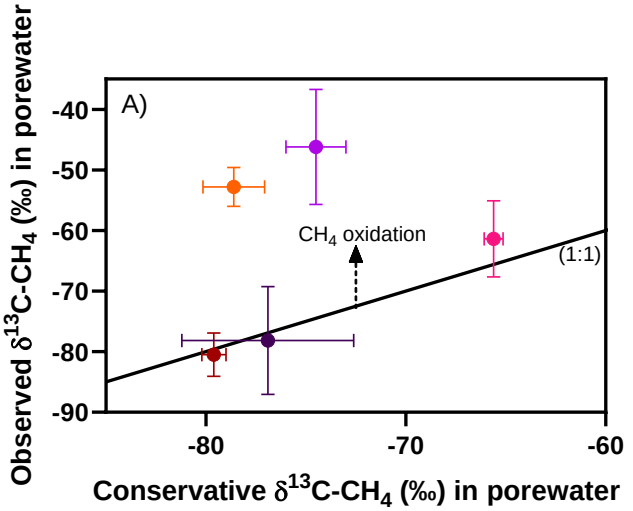
A)
CH4 oxidation
(1:1)
Observed δ13C-CH4 (‰) in porewater
Conservative δ13C-CH4 (‰) in porewater
-40
-50
-60
-70
-80
-90
-80
-70
-60

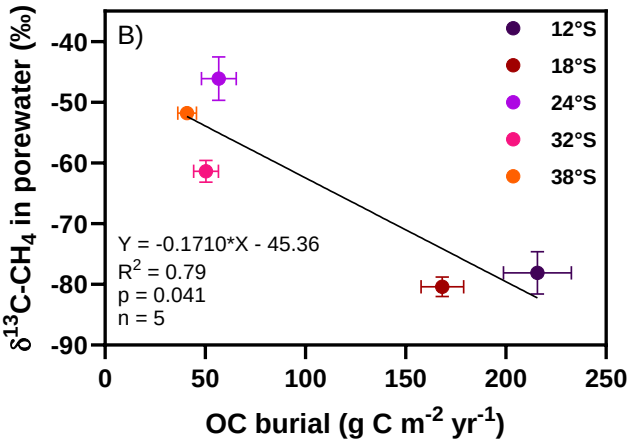
B)
12°S
18°S
24°S
32°S
38°S
Y = -0.1710*X - 45.36
R2 = 0.79
p = 0.041
n = 5
δ13C-CH4 in porewater (‰)
OC burial (g C m-2 yr-1)
-40
-50
-60
-70
-80
-90
0
50
100
150
200
250

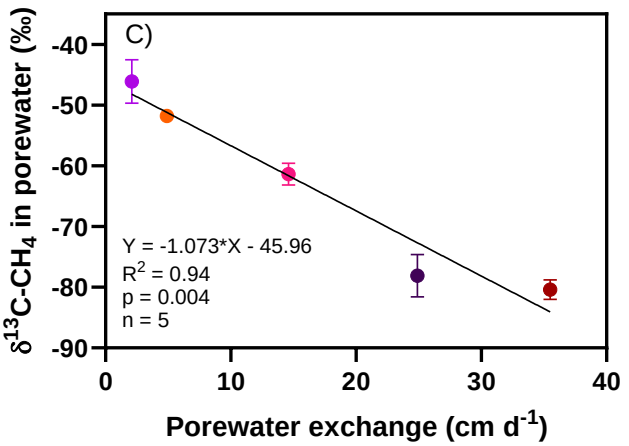
C)
Y = -1.073*X - 45.96
R2 = 0.94
p = 0.004
n = 5
δ13C-CH4 in porewater (‰)
Porewater exchange (cm d-1)
-40
-50
-60
-70
-80
-90
0
10
20
30
40

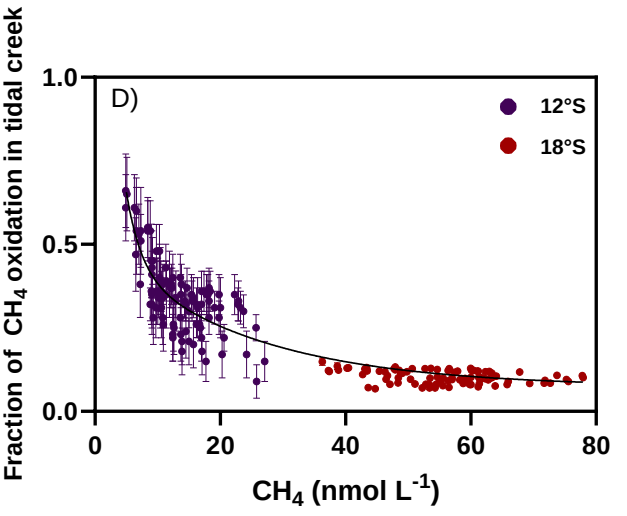
D)
12°S
18°S
Fraction of CH4 oxidation in tidal creek
CH4 (nmol L-1)
1.0
0.5
0.0
0
20
40
60
80

CH_4 emissions (CO_2e, $SGWP_{20}$, Tg CO_2 $year^{-1}$) in global mangroves